Double Helicity Asymmetry in Inclusive Midrapidity π^0 Production for Polarized $p + p$ Collisions at $\sqrt{s} = 200$ GeV

S. S. Adler,[5] S. Afanasiev,[20] C. Aidala,[10] N. N. Ajitanand,[44] Y. Akiba,[21,40] A. Al-Jamel,[35] J. Alexander,[44] K. Aoki,[25] L. Aphecetche,[46] R. Armendariz,[35] S. H. Aronson,[5] R. Averbeck,[45] T. C. Awes,[36] V. Babintsev,[17] A. Baldisseri,[11] K. N. Barish,[6] P. D. Barnes,[28] B. Bassalleck,[34] S. Bathe,[6,31] S. Batsouli,[10] V. Baublis,[39] F. Bauer,[6] A. Bazilevsky,[5,41] S. Belikov,[19,17] M. T. Bjorndal,[10] J. G. Boissevain,[28] H. Borel,[11] M. L. Brooks,[28] D. S. Brown,[35] N. Bruner,[34] D. Bucher,[31] H. Buesching,[5,31] V. Bumazhnov,[17] G. Bunce,[5,41] J. M. Burward-Hoy,[28,27] S. Butsyk,[45] X. Camard,[46] P. Chand,[4] W. C. Chang,[2] S. Chernichenko,[17] C. Y. Chi,[10] J. Chiba,[21] M. Chiu,[10] I. J. Choi,[53] R. K. Choudhury,[4] T. Chujo,[5] V. Cianciolo,[36] Y. Cobigo,[11] B. A. Cole,[10] M. P. Comets,[37] P. Constantin,[19] M. Csanád,[13] T. Csörgő,[22] J. P. Cussonneau,[46] D. d'Enterria,[10] K. Das,[14] G. David,[5] F. Deák,[13] H. Delagrange,[46] A. Denisov,[17] A. Deshpande,[41] E. J. Desmond,[5] A. Devismes,[45] O. Dietzsch,[42] J. L. Drachenberg,[1] O. Drapier,[26] A. Drees,[45] A. Durum,[17] D. Dutta,[4] V. Dzhordzhadze,[47] Y. V. Efremenko,[36] H. En'yo,[40,41] B. Espagnon,[37] S. Esumi,[49] D. E. Fields,[34,41] C. Finck,[46] F. Fleuret,[26] S. L. Fokin,[24] B. D. Fox,[41] Z. Fraenkel,[52] J. E. Frantz,[10] A. Franz,[5] A. D. Frawley,[14] Y. Fukao,[25,40,41] S.-Y. Fung,[6] S. Gadrat,[29] M. Germain,[46] A. Glenn,[47] M. Gonin,[26] J. Gosset,[11] Y. Goto,[40,41] R. Granier de Cassagnac,[26] N. Grau,[19] S. V. Greene,[50] M. Grosse Perdekamp,[18,41] H.-Å. Gustafsson,[30] T. Hachiya,[16] J. S. Haggerty,[5] H. Hamagaki,[8] A. G. Hansen,[28] E. P. Hartouni,[27] M. Harvey,[5] K. Hasuko,[40] R. Hayano,[8] X. He,[15] M. Heffner,[27] T. K. Hemmick,[45] J. M. Heuser,[40] P. Hidas,[22] H. Hiejima,[18] J. C. Hill,[19] R. Hobbs,[34] W. Holzmann,[44] K. Homma,[16] B. Hong,[23] A. Hoover,[35] T. Horaguchi,[40,41,48] T. Ichihara,[40,41] V. V. Ikonnikov,[24] K. Imai,[25,40] M. Inaba,[49] M. Inuzuka,[8] D. Isenhower,[1] L. Isenhower,[1] M. Ishihara,[40] M. Issah,[44] A. Isupov,[20] B. V. Jacak,[45] J. Jia,[45] O. Jinnouchi,[40,41] B. M. Johnson,[5] S. C. Johnson,[27] K. S. Joo,[32] D. Jouan,[37] F. Kajihara,[8] S. Kametani,[8,51] N. Kamihara,[40,48] M. Kaneta,[41] J. H. Kang,[53] K. Katou,[51] T. Kawabata,[8] A. Kazantsev,[24] S. Kelly,[9,10] B. Khachaturov,[52] A. Khanzadeev,[39] J. Kikuchi,[51] D. J. Kim,[53] E. Kim,[43] G.-B. Kim,[26] H. J. Kim,[53] E. Kinney,[9] A. Kiss,[13] E. Kistenev,[5] A. Kiyomichi,[40] C. Klein-Boesing,[31] H. Kobayashi,[41] V. Kochetkov,[17] R. Kohara,[16] B. Komkov,[39] M. Konno,[49] D. Kotchetkov,[6] A. Kozlov,[52] P. J. Kroon,[5] C. H. Kuberg,[1] G. J. Kunde,[28] K. Kurita,[40] M. J. Kweon,[23] Y. Kwon,[53] G. S. Kyle,[35] R. Lacey,[44] J. G. Lajoie,[19] Y. Le Bornec,[37] A. Lebedev,[19,24] S. Leckey,[45] D. M. Lee,[28] M. J. Leitch,[28] M. A. L. Leite,[42] X. Li,[7] X. H. Li,[6] H. Lim,[43] A. Litvinenko,[20] M. X. Liu,[28] C. F. Maguire,[50] Y. I. Makdisi,[5] A. Malakhov,[20] V. I. Manko,[24] Y. Mao,[38,40] G. Martinez,[46] H. Masui,[49] F. Matathias,[45] T. Matsumoto,[8,51] M. C. McCain,[1] P. L. McGaughey,[28] Y. Miake,[49] T. E. Miller,[50] A. Milov,[45] S. Mioduszewski,[5] G. C. Mishra,[15] J. T. Mitchell,[5] A. K. Mohanty,[4] D. P. Morrison,[5] J. M. Moss,[28] D. Mukhopadhyay,[52] M. Muniruzzaman,[6] S. Nagamiya,[21] J. L. Nagle,[9,10] T. Nakamura,[16] J. Newby,[47] A. S. Nyanin,[24] J. Nystrand,[30] E. O'Brien,[5] C. A. Ogilvie,[19] H. Ohnishi,[40] I. D. Ojha,[3,50] H. Okada,[25,40] K. Okada,[40,41] A. Oskarsson,[30] I. Otterlund,[30] K. Oyama,[8] K. Ozawa,[8] D. Pal,[52] A. P. T. Palounek,[28] V. Pantuev,[45] V. Papavassiliou,[35] J. Park,[43] W. J. Park,[23] S. F. Pate,[35] H. Pei,[19] V. Penev,[20] J.-C. Peng,[18] H. Pereira,[11] V. Peresedov,[20] A. Pierson,[34] C. Pinkenburg,[5] R. P. Pisani,[5] M. L. Purschke,[5] A. K. Purwar,[45] J. Qualls,[1] J. Rak,[19] I. Ravinovich,[52] K. F. Read,[36,47] M. Reuter,[45] K. Reygers,[31] V. Riabov,[39] Y. Riabov,[39] G. Roche,[29] A. Romana,[26] M. Rosati,[19] S. Rosendahl,[30] P. Rosnet,[29] V. L. Rykov,[40] S. S. Ryu,[53] N. Saito,[25,40,41] T. Sakaguchi,[8,51] S. Sakai,[49] V. Samsonov,[39] L. Sanfratello,[34] R. Santo,[31] H. D. Sato,[25,40] S. Sato,[5,49] S. Sawada,[21] Y. Schutz,[46] V. Semenov,[17] R. Seto,[6] T. K. Shea,[5] I. Shein,[17] T.-A. Shibata,[40,48] K. Shigaki,[16] M. Shimomura,[49] A. Sickles,[45] C. L. Silva,[42] D. Silvermyr,[28] K. S. Sim,[23] A. Soldatov,[17] R. A. Soltz,[27] W. E. Sondheim,[28] S. Sorensen,[47] I. V. Sourikova,[5] F. Staley,[11] P. W. Stankus,[36] E. Stenlund,[30] M. Stepanov,[35] A. Ster,[22] S. P. Stoll,[5] T. Sugitate,[16] J. P. Sullivan,[28] S. Takagi,[49] E. M. Takagui,[42] A. Taketani,[40,41] K. H. Tanaka,[21] Y. Tanaka,[33] K. Tanida,[40] M. J. Tannenbaum,[5] A. Taranenko,[44] P. Tarján,[12] T. L. Thomas,[34] M. Togawa,[25,40] J. Tojo,[40] H. Torii,[25,41] R. S. Towell,[1] V-N. Tram,[26] I. Tserruya,[52] Y. Tsuchimoto,[16] H. Tydesjö,[30] N. Tyurin,[17] T. J. Uam,[32] H. W. van Hecke,[28] J. Velkovska,[5] M. Velkovsky,[45] V. Veszprémi,[12] A. A. Vinogradov,[24] M. A. Volkov,[24] E. Vznuzdaev,[39] X. R. Wang,[15] Y. Watanabe,[40,41] S. N. White,[5] N. Willis,[37] F. K. Wohn,[19] C. L. Woody,[5] W. Xie,[6] A. Yanovich,[17] S. Yokkaichi,[40,41] G. R. Young,[36] I. E. Yushmanov,[24] W. A. Zajc,[10,*] O. Zaudtke,[31] C. Zhang,[10] S. Zhou,[7] J. Zimányi,[22] L. Zolin,[20] and X. Zong[19]

(PHENIX Collaboration)

[1]*Abilene Christian University, Abilene, Texas 79699, USA*
[2]*Institute of Physics, Academia Sinica, Taipei 11529, Taiwan*
[3]*Department of Physics, Banaras Hindu University, Varanasi 221005, India*

 0031-9007/04/93(20)/202002(6)$22.50

[4]*Bhabha Atomic Research Centre, Bombay 400 085, India*
[5]*Brookhaven National Laboratory, Upton, New York 11973-5000, USA*
[6]*University of California–Riverside, Riverside, California 92521, USA*
[7]*China Institute of Atomic Energy (CIAE), Beijing, People's Republic of China*
[8]*Center for Nuclear Study, Graduate School of Science, University of Tokyo, 7-3-1 Hongo, Bunkyo, Tokyo 113-0033, Japan*
[9]*University of Colorado, Boulder, Colorado 80309, USA*
[10]*Columbia University, New York, New York 10027, USA,*
and Nevis Laboratories, Irvington, New York 10533, USA
[11]*Dapnia, CEA Saclay, F-91191, Gif-sur-Yvette, France*
[12]*Debrecen University, H-4010 Debrecen, Egyetem tér 1, Hungary*
[13]*ELTE, Eötvös Loránd University, H-1117 Budapest, Pázmány P. s. 1/A, Hungary*
[14]*Florida State University, Tallahassee, Florida 32306, USA*
[15]*Georgia State University, Atlanta, Georgia 30303, USA*
[16]*Hiroshima University, Kagamiyama, Higashi-Hiroshima 739-8526, Japan*
[17]*Institute for High Energy Physics (IHEP), Protvino, Russia*
[18]*University of Illinois at Urbana-Champaign, Urbana, Illinois 61801, USA*
[19]*Iowa State University, Ames, Iowa 50011, USA*
[20]*Joint Institute for Nuclear Research, 141980 Dubna, Moscow Region, Russia*
[21]*KEK, High Energy Accelerator Research Organization, Tsukuba-shi, Ibaraki-ken 305-0801, Japan*
[22]*KFKI Research Institute for Particle and Nuclear Physics (RMKI), H-1525 Budapest 114, POBox 49, Hungary*
[23]*Korea University, Seoul, 136-701, Korea*
[24]*Russian Research Center "Kurchatov Institute," Moscow, Russia*
[25]*Kyoto University, Kyoto 606-8394, Japan*
[26]*Laboratoire Leprince-Ringuet, Ecole Polytechnique, CNRS-IN2P3, Route de Saclay, F-91128, Palaiseau, France*
[27]*Lawrence Livermore National Laboratory, Livermore, California 94550, USA*
[28]*Los Alamos National Laboratory, Los Alamos, New Mexico 87545, USA*
[29]*LPC, Université Blaise Pascal, CNRS-IN2P3, Clermont-Fd, 63177 Aubiere Cedex, France*
[30]*Department of Physics, Lund University, Box 118, SE-221 00 Lund, Sweden*
[31]*Institut fuer Kernphysik, University of Muenster, D-48149 Muenster, Germany*
[32]*Myongji University, Yongin, Kyonggido 449-728, Korea*
[33]*Nagasaki Institute of Applied Science, Nagasaki-shi, Nagasaki 851-0193, Japan*
[34]*University of New Mexico, Albuquerque, New Mexico 87131, USA*
[35]*New Mexico State University, Las Cruces, New Mexico 88003, USA*
[36]*Oak Ridge National Laboratory, Oak Ridge, Tennessee 37831, USA*
[37]*IPN-Orsay, Universite Paris Sud, CNRS-IN2P3, BP1, F-91406, Orsay, France*
[38]*Peking University, Beijing, People's Republic of China*
[39]*PNPI, Petersburg Nuclear Physics Institute, Gatchina, Russia*
[40]*RIKEN (The Institute of Physical and Chemical Research), Wako, Saitama 351-0198, Japan*
[41]*RIKEN BNL Research Center, Brookhaven National Laboratory, Upton, New York 11973-5000, USA*
[42]*Universidade de São Paulo, Instituto de Física, Caixa Postal 66318, São Paulo CEP05315-970, Brazil*
[43]*System Electronics Laboratory, Seoul National University, Seoul, South Korea*
[44]*Chemistry Department, Stony Brook University, SUNY, Stony Brook, New York 11794-3400, USA*
[45]*Department of Physics and Astronomy, Stony Brook University, SUNY, Stony Brook, New York 11794, USA*
[46]*SUBATECH (Ecole des Mines de Nantes, CNRS-IN2P3, Université de Nantes), BP 20722-44307, Nantes, France*
[47]*University of Tennessee, Knoxville, Tennessee 37996, USA*
[48]*Department of Physics, Tokyo Institute of Technology, Tokyo, 152-8551, Japan*
[49]*Institute of Physics, University of Tsukuba, Tsukuba, Ibaraki 305, Japan*
[50]*Vanderbilt University, Nashville, Tennessee 37235, USA*
[51]*Waseda University, Advanced Research Institute for Science and Engineering, 17 Kikui-cho, Shinjuku-ku, Tokyo 162-0044, Japan*
[52]*Weizmann Institute, Rehovot 76100, Israel*
[53]*Yonsei University, IPAP, Seoul 120-749, Korea*
(Received 21 April 2004; published 11 November 2004)

We present a measurement of the double longitudinal spin asymmetry in inclusive π^0 production in polarized proton-proton collisions at $\sqrt{s} = 200$ GeV. The data were taken at the Relativistic Heavy Ion Collider with average beam polarizations of 0.27. The measurements are the first in a program to study the longitudinal spin structure of the proton, using strongly interacting probes, at collider energies. The asymmetry is presented for transverse momenta 1–5 GeV/c at midrapidity, where next-to-leading-order perturbative quantum chromodynamic (NLO pQCD) calculations well describe the unpolarized cross section. The observed asymmetry is small and is compared to a NLO pQCD calculation with a range of polarized gluon distributions.

DOI: 10.1103/PhysRevLett.93.202002 PACS numbers: 13.85.Ni, 13.88.+e, 21.10.Hw, 25.40.Fq

From polarized lepton-nucleon deep inelastic scattering (DIS) experiments over the past 20 years it is known that only ~25% of the proton spin can be attributed to the spins of the quarks and antiquarks [1]. The rest of the proton spin must hence be carried by the gluons and orbital angular momentum. DIS experiments have constrained the possible gluon polarization in the proton through the measurement of scaling violation in inclusive polarized scattering [2], and through semi-inclusive measurements of two hadrons to utilize the photon-gluon fusion process [3]. A fixed target experiment at Fermilab first presented a measurement with strongly interacting probes [4]. The reach of these measurements was limited, due to the low energy available for fixed target experiments. Presently, the gluon contribution to the proton spin is largely unknown.

The polarized proton collisions at the Relativistic Heavy Ion Collider (RHIC) provide a new laboratory to study the proton spin structure with strongly interacting probes. The PHENIX experiment has reported the unpolarized cross section for π^0 production at midrapidity for $p_T = 1$–14 GeV/c, which is described well by next-to-leading-order perturbative QCD (NLO pQCD) calculations over 8 orders of magnitude [5]. In this Letter we report the first results on the double spin asymmetry A_{LL} for inclusive π^0 production at midrapidity in longitudinally polarized proton-proton collisions corresponding to $0.22\ \mathrm{pb}^{-1}$ integrated luminosity with the PHENIX detector.

In perturbative QCD A_{LL} is directly sensitive to the polarized gluon distribution function in the proton through gluon-gluon and gluon-quark subprocesses [6,7].

The double spin asymmetry in π^0 production is given by

$$A_{LL}^{\pi^0} = \frac{\sigma_{++} - \sigma_{+-}}{\sigma_{++} + \sigma_{+-}}, \tag{1}$$

where σ_{++} (σ_{+-}) is the cross section of the reaction when two colliding particles have the same (opposite) helicity. Here we neglect the parity violating difference in cross section between $(++) \leftrightarrow (--)$ and $(+-) \leftrightarrow (-+)$ beam helicity configurations. Since the cross section can be obtained by dividing the experimental yield (N) by the integrated luminosity (L), A_{LL} is expressed as

$$A_{LL} = \frac{1}{|\langle P_B P_Y \rangle|} \frac{N_{++} - R N_{+-}}{N_{++} + R N_{+-}}; \qquad R = \frac{L_{++}}{L_{+-}}, \tag{2}$$

where $P_{Y(B)}$ are the polarizations of the RHIC "yellow" ("blue") beams, and R is the ratio of luminosities of protons colliding with like to unlike helicities.

For the 2002–2003 RHIC run, 55 bunches of polarized protons, typically 5×10^{10} protons per bunch, were loaded into each of the yellow and blue accelerator/storage rings of RHIC and accelerated to 100 GeV. The bunch lengths and separations were ~1 and 213 ns, respectively. The beam polarization sign for each bunch was prepared independently at the source, with the successive bunches in one ring alternating in polarization sign, and with successive pairs of bunches in the other ring alternating in sign. The locations of the bunches were identified relative to a RHIC timing clock. In this way, the experiments collected data from collisions with all four combinations of blue-yellow ring beam polarization signs simultaneously.

The stable direction of the proton spin in RHIC is vertical, but the region around the PHENIX experiment includes sets of magnets (spin rotators) to rotate the spin to the longitudinal direction at the collision point, and then back to vertical after the interaction point, in order to provide collisions with longitudinal polarization, and to maintain the required vertical polarization around RHIC. The RHIC polarimeters measure the transverse beam polarization away from the interaction points, independent of the operation of the spin rotators.

The transverse beam polarization was measured in RHIC independently in each beam using proton-carbon elastic scattering in the Coulomb nuclear interference region [8]. The analyzing power A_N^{pC} was measured for 22 GeV beam energy, $A_N^{pC}(22)$, to ±30% [9]. The energy dependence of the analyzing power over the RHIC energies is expected to be small, <10% [10]. For the results reported here, we have used the same analyzing power at 100 GeV as at 22 GeV, and 10% is added in quadrature to the relative uncertainty for $A_N^{pC}(22)$ to give a ±32% uncertainty for $A_N^{pC}(100)$. With these assumptions, the average polarization in the analyzed data set in this paper was $\sqrt{\langle P_B P_Y \rangle} = 0.27 \pm 1\%(\mathrm{stat}) \pm 10\%(\mathrm{syst}) \pm 32\%(A_N^{pC}\ \mathrm{syst})$.

Local polarimeters, sensitive to the transverse polarization at collision, were used to set up the spin rotators, and to monitor the beam polarization direction at the PHENIX experiment. The local polarimeters utilized a transverse single-spin asymmetry in neutron production in p-p collisions at $\sqrt{s} = 200$ GeV [11]. For vertically polarized beam a left-right asymmetry is observed for neutrons produced at very forward angles, with no asymmetry for production at very backward angles. A fully longitudinally polarized beam produces no asymmetry.

Neutrons with $E_n > 20$ GeV and production angle $0.3 < \theta_n < 2.5$ mrad were observed by two hadronic calorimeters located ±18 m from the interaction point [zero degree calorimeter (ZDC) [12]]. Scintillator hodoscopes at 1.7 interaction length provided the neutron position at the ZDC, and thus the neutron production angle and azimuthal angle $\phi = \arctan(x/y)$ with $\hat{y}$ vertically upward. The $\hat{x}$ axis forms a right-handed coordinate system with the $\hat{z}$ axis defined by the beam direction for forward

production. The single-spin asymmetry ϵ was calculated versus azimuth, from the four rates $N_{\uparrow,\phi}$, $N_{\uparrow,\phi+\pi}$, $N_{\downarrow,\phi}$, $N_{\downarrow,\phi+\pi}$, using the geometric mean [13]. This method largely cancels differences in luminosity between $\uparrow$ and $\downarrow$ polarization collisions and between detector acceptance differences at ϕ and $\phi + \pi$. Figure 1 shows the observed asymmetry, for the spin rotators off and on, for the blue and yellow beams. With the spin rotators off, a left-right asymmetry is observed from the vertically polarized beam. With the spin rotators on, the measured transverse polarization, averaged over the run, was $\langle P_{Bx}\rangle = 0.033 \pm 0.019$, $\langle P_{By}\rangle = 0.008 \pm 0.020$, $\langle P_{Yx}\rangle = -0.020 \pm 0.013$, and $\langle P_{Yy}\rangle = 0.054 \pm 0.017$, out of $\langle P\rangle = 0.27$. The double spin transverse polarization was $\langle P_{Bx}P_{Yx}\rangle = (0.4 \pm 1.1) \times 10^{-3}$ and $\langle P_{By}P_{Yy}\rangle = (-0.2 \pm 0.8) \times 10^{-3}$, compared to $\langle P_B P_Y\rangle = 0.07$. Therefore, with the spin rotators on, the transverse asymmetry is greatly reduced, indicating a high degree of longitudinal polarization: the longitudinal fraction of the beam polarization was 0.99 and 0.98 for the blue and yellow beams, respectively.

A separate run with the spin rotators set to give radial polarization confirmed the direction of the polarization for each beam.

Collisions in PHENIX are defined by the coincidence of signals in two beam-beam counters (BBC) [14] located ± 1.44 m from the nominal interaction point and subtending a pseudorapidity range $\pm(3.0$–$3.9)$ with full azimuthal coverage. The BBCs select about half of the inelastic proton-proton collisions [5]. The vertex was reconstructed from the time difference of the hits in the two BBCs. The collision vertex was required to be within 30 cm of the nominal interaction point. Events satisfying this condition constitute the minimum bias (MB) trigger, which was used for relative luminosity measurements.

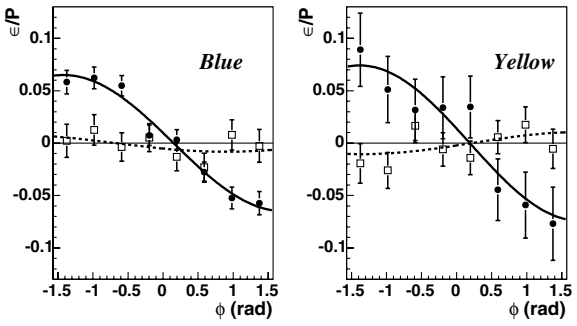

FIG. 1. The raw asymmetry normalized by the beam polarization ϵ/P as a function of azimuthal angle ϕ, for forward neutron production. The solid points and curve correspond to the spin rotators off (transverse polarization) and the open points and dashed curve correspond to the spin rotators on (longitudinal polarization). Curves are sine function fits to the data, representing possible transverse polarization. The data are for special runs used to set up the spin rotators, where the blue (yellow) polarization was 0.24 and 0.33 (0.08 and 0.28), for spin rotators off and on, correspondingly.

A coincidence of the two ZDCs was used to estimate the possible bias in the relative luminosity measurement from the BBCs. This was done by comparing the accumulated number of triggers in the ZDCs and BBCs for each bunch and each fill. The accuracy of relative luminosity measurements δR [Eq. (2)] was estimated to be 2.5×10^{-4}, which for the average beam polarization of 0.27 translated to $\delta A_{LL} = 1.8 \times 10^{-3}$, and, on the same uncertainty level, confirmed no A_{LL} asymmetry of BBC triggers relative to ZDC. The ratio R averaged over the data sample used in the analysis was within 0.5% of unity.

Neutral pions were reconstructed from the $\pi^0 \to \gamma\gamma$ decays using finely granulated ($\Delta\phi \times \Delta\eta \sim 0.01 \times 0.01$) electromagnetic calorimeters (EMCal) [15], which consisted of two subsystems: a lead scintillator (PbSc) and a lead glass (PbGl) calorimeter covering three quarters and one quarter of the EMCal acceptance, respectively. Located at a radial distance of $\sim$5 m from the beam line, the EMCal covered the pseudorapidity range of $|\eta| < 0.35$ and two azimuthal angle intervals of $\Delta\phi \approx 90°$ separated by $\phi \approx 70°$ (nearly back-to-back).

High p_T π^0's were collected using coincidences between a MB trigger and an EMCal-based high p_T photon trigger [5]. The trigger efficiency for π^0's varied from 8% in the 1–2 GeV/c p_T bin to 90% in the 4–5 GeV/c p_T bin.

The π^0 reconstruction and photon identification cuts were optimized to minimize the background contribution under the π^0 peak in the invariant mass distribution while keeping the π^0 efficiency high. For photon identification we used the shower shape and the time of flight measured by the EMCal, and charge veto cuts. The charge veto was set for those EMCal clusters associated with hit(s) in the pad chamber [16], which was located $\sim$20 cm in front of the EMCal surface. In order to avoid the effects of electronic noise and to suppress the very low energy background, only clusters with energy greater than 0.1 GeV in PbSc and 0.2 GeV in PbGl were used in the analysis.

The π^0 yield was extracted by integrating the two photon invariant mass spectrum over a ± 25 MeV/c^2 region around the π^0 mass (signal region). The EMCal resolution was such that the widths of the π^0 mass peaks varied from 12 MeV/c^2 in the 1–2 GeV/c p_T bin to 9.5 MeV/c^2 in the 4–5 GeV/c p_T bin, in both PbSc and PbGl. In the p_T range of 1 to 5 GeV/c, 4×10^6 π^0 candidates were collected. The background contribution (combinatorial + hadronic) under the π^0 peak r varied from 27% in the 1–2 GeV/c bin to 8% in the 4–5 GeV/c bin. The π^0 reconstruction efficiency due to photon identification cuts varied from 84% in the lowest p_T bin to 93% in the highest p_T bin.

The asymmetry of the background in the signal region A_{LL}^{BG} was evaluated using the asymmetry calculated from the data in $\gamma\gamma$ mass regions 50 MeV/c^2 wide on either side of the π^0 peak, centered at masses 75 and

195 MeV/c^2. The measured π^0 asymmetry $A_{LL}^{\rm raw}$ was corrected for the contribution of background using

$$A_{LL}^{\pi^0} = \frac{A_{LL}^{\rm raw} - rA_{LL}^{BG}}{1-r}, \qquad \sigma_{A_{LL}^{\pi^0}} = \frac{\sqrt{\sigma^2_{A_{LL}^{\rm raw}} + r^2\sigma^2_{A_{LL}^{BG}}}}{1-r}. \quad (3)$$

The spin asymmetry for each beam fill [17] $A_{LL}^{\rm fill}$ was calculated using Eq. (2). For the $A_{LL}^{\rm fill}$ error evaluation, we considered only the N_{++} and N_{+-} statistical errors. The resulting A_{LL} was obtained after fitting a constant to all $A_{LL}^{\rm fill}$'s. The fit $\chi^2_{\rm fit}$ and a "bunch shuffling" technique were used to evaluate the uncertainties assigned to A_{LL}. In each bunch shuffling we randomly assigned the helicity sign to every bunch crossing, keeping the balance between the number of bunches with correctly and inversely assigned helicities, so that the average polarization for each shuffled sample was nearly zero, and recalculated A_{LL}. The widths of the distributions of A_{LL} values obtained in all bunch shuffles were consistent with errors assigned to A_{LL} indicating that all noncorrelated bunch-to-bunch and fill-to-fill systematic errors were much smaller than the π^0 yield statistical errors.

A number of systematic checks, including variation of photon identification criteria and mass window range for π^0's and background, were performed to look for possible systematic effects on the measured A_{LL} values. None were found.

The double spin asymmetries between $(++)$ and $(--)$ and between $(+-)$ and $(-+)$ helicity configurations, as well as the single-spin asymmetries for each polarized beam ($A_L = -\frac{\sigma_+ - \sigma_-}{\sigma_+ + \sigma_-}$) were evaluated. These measure parity violating asymmetries, if any. All of these asymmetries were consistent with zero.

The results are presented in Table I and Fig. 2. Systematic uncertainties for the asymmetry measurements are negligible. A total scale uncertainty of $\pm 65\%$, from the correlated polarization analyzing power uncertainty δA_N^{pC} for the two beams and the uncorrelated measurement uncertainties, is not shown.

Two theoretical curves based on NLO pQCD are shown in Fig. 2, representing different assumptions for the gluon polarization, one using the best global fit to inclusive DIS data (GRSV-std), and another one using a gluon polarized distribution equal to the unpolarized distribution at the input scale of $Q^2 = 0.6$ GeV^2 (GRSV-max) [6,18]. The gluon polarization contributes to A_{LL} through gluon-gluon and gluon-quark subprocesses, with the gluon-gluon contribution significantly larger at midrapidity and for the estimated gluon momentum fraction for these results $x \approx 0.03$–0.1 [19]. Thus, the asymmetry A_{LL} is approximately proportional to the square of the gluon polarization and a negative value of A_{LL} is not expected [20]. The results are consistent with zero or small gluon polarization, with a confidence level (C.L.) of 16%–20% for GRSV-std, for the range in polarization uncertainty of the measurement. The results are less consistent with a large gluon polarization, with C.L. = 0.02%–5% for GRSV-max.

We emphasize the following points: (1) The lowest p_T point reported here can have a significant contribution from soft physics, since the agreement of the NLO pQCD calculation with the measured cross section [5] can only be checked to within the uncertainties of the calculation, estimated to be a factor two at this p_T [6,20]. If the soft physics is represented by an exponential falloff in p_T (e^{-6p_T} is typically used [21]), the soft physics contribution to the higher p_T data is small ($< 10\%$ to the 2–3 GeV/c p_T bin if we assume equal soft/hard contributions to the lowest bin). If we consider only the highest three p_T bins, the C.L. = 58%–67% for GRSV-std, and C.L. = 0.4%–29% for GRSV-max. (2) These confidence levels do not include a theoretical uncertainty, from either scales or from choices of parton distribution functions and fragmentation function. The comparisons are made for NLO pQCD, rather than extracting a leading-order estimate of the gluon polarization. (3) The range of theory curves in Fig. 2 reflects the uncertainty on gluon polarization from inclusive DIS measurements [18,22–24].

In summary, we have presented a new technique for determining the polarized gluon distribution using polarized protons acting as strongly interacting probes, at

TABLE I. Double and single-spin asymmetries for four p_T bins with mean $p_T(\pi^0)$ 1.59, 2.39, 3.37, and 4.38 GeV/c.

p_T (GeV/c)	$A_{LL}^{\rm raw}$ (10^{-2})	A_{LL}^{BG} (10^{-2})	$A_{LL}^{\pi^0}$ (10^{-2})	$A_L^{\pi^0}$ (10^{-2})
1–2	-1.5 ± 0.9	1.6 ± 1.4	-2.7 ± 1.3	-0.2 ± 0.3
2–3	-1.5 ± 1.1	-3.0 ± 2.4	-1.3 ± 1.3	-0.1 ± 0.3
3–4	-1.8 ± 2.5	-2.4 ± 6.8	-1.7 ± 2.8	-0.3 ± 0.6
4–5	2.6 ± 5.7	24 ± 17	0.7 ± 6.2	-1.0 ± 1.2

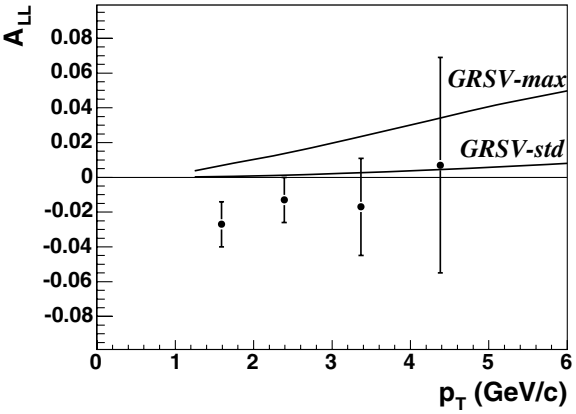

FIG. 2. $A_{LL}^{\pi^0}$ versus mean p_T of π^0's in each bin. A scale uncertainty of $\pm 65\%$ is not included. Two theoretical calculations based on NLO pQCD are also shown for comparison with the data (see text for details).

collider energies. The reported results of the double spin helicity asymmetries for π^0 production begin to probe the proton spin structure in the perturbative QCD regime with a sensitivity comparable to the polarized inclusive deep inelastic scattering data. The observed asymmetry is small and consistent with a small gluon polarization.

We thank the staff of the Collider-Accelerator Department, Magnet Division, and Physics Department at BNL and the RHIC polarimetry group for their vital contributions. We thank W. Vogelsang for informative discussions. We acknowledge support from the Department of Energy and NSF (U.S.A.), MEXT and JSPS (Japan), CNPq and FAPESP (Brazil), NSFC (China), IN2P3/CNRS, CEA, and ARMINES (France), BMBF, DAAD, and AvH (Germany), OTKA (Hungary), DAE and DST (India), ISF (Israel), KRF and CHEP (Korea), RAS, RMAE, and RMS (Russia), VR and KAW (Sweden), U.S. CRDF for the FSU, U.S.-Hungarian NSF-OTKA-MTA, and U.S.-Israel BSF.

*PHENIX Spokesperson.
Electronic address: zajc@nevis.columbia.edu

[1] J. Ashman *et al.*, Phys. Lett. B **206**, 364 (1988); Nucl. Phys. **B328**, 1 (1989); E. Hughes and R. Voss, Annu. Rev. Nucl. Part. Sci. **49**, 303 (1999).
[2] B. Adeva *et al.*, Phys. Rev. D **58**, 112002 (1998); P. L. Anthony *et al.*, Phys. Lett. B **493**, 19 (2000).
[3] A. Airapetian *et al.*, Phys. Rev. Lett. **84**, 2584 (2000); B. Adeva *et al.*, Phys. Rev. D **70**, 012002 (2004).
[4] D. L. Adams *et al.*, Phys. Lett. B **261**, 197 (1991).
[5] S. S. Adler *et al.*, Phys. Rev. Lett. **91**, 241803 (2003).
[6] B. Jäger, A. Schafer, M. Stratmann, and W. Vogelsang, Phys. Rev. D **67**, 054005 (2003).
[7] B. Jäger *et al.*, in the Proceedings of the 8th Workshop on High Energy Physics Phenomenology (WHEPP 8), Bombay, India, 2004 (to be published); hep-ph/0405069.
[8] O. Jinnouchi *et al.*, RHIC/CAD Accelerator Physics Note 171, 2004.
[9] J. Tojo *et al.*, Phys. Rev. Lett. **89**, 052302 (2002).
[10] T. L. Trueman, hep-ph/0203013.
[11] A. Bazilevsky *et al.*, in *SPIN 2002: 15th International Spin Physics Symposium and Workshop on Polarized Electron Sources and Polarimeters*, AIP Conf. Proc. 675 (AIP, New York, 2003), pp. 584–588.
[12] C. Adler *et al.*, Nucl. Instrum. Methods Phys. Res., Sect. A **470**, 488 (2001).
[13] G. G. Ohlsen and P. W. Keaton, Jr., Nucl. Instrum. Methods **109**, 41 (1973).
[14] M. Allen *et al.*, Nucl. Instrum. Methods Phys. Res., Sect. A **499**, 549 (2003).
[15] L. Aphecetche *et al.*, Nucl. Instrum. Methods Phys. Res., Sect. A **499**, 521 (2003).
[16] K. Adcox *et al.*, Nucl. Instrum. Methods Phys. Res., Sect. A **499**, 489 (2003).
[17] Each fill is characterized by a constant polarization of the beams.
[18] M. Glück, E. Reya, M. Stratmann, and W. Vogelsang, Phys. Rev. D **63**, 094005 (2001).
[19] B. Jäger, M. Stratmann, and W. Vogelsang, Phys. Rev. D **70**, 034010 (2004).
[20] B. Jäger, M. Stratmann, S. Kretzer, and W. Vogelsang, Phys. Rev. Lett. **92**, 121803 (2004).
[21] S. M. Berman, J. D. Bjorken, and J. B. Kogut, Phys. Rev. D **4**, 3388 (1971).
[22] J. Blümlein and H. Böttcher, Nucl. Phys. **B636**, 225 (2002).
[23] M. Hirai, S. Kumano, and N. Saito, Phys. Rev. D **69**, 054021 (2004).
[24] M. Hirai and K. Sudoh, hep-ph/0403102; RIKEN Report No. RIKEN-AF-NP-456.